RESEARCH ARTICLE

Journal of RAMAN SPECTROSCOPY WILEY

Corroborating the autoptic identification of archeological glyptics in museum collections: The contribution of portable Raman spectroscopy

Maria Cristina Caggiani[1] [iD] | Marco Cavarra[1] [iD] | Germana Barone[1] [iD] |
Alessia Coccato[2] [iD] | Angela Maria Manenti[3] | Paolo Mazzoleni[1] [iD]

[1]Department of Biological, Geological and Environmental Sciences, University of Catania, Catania, Italy

[2]Faculty of Classics, Ioannou Centre for Classical and Byzantine Studies, University of Oxford, Oxford, UK

[3]Parco Archeologico e Paesaggistico di Siracusa, Eloro, Villa del Tellaro e Akrai, Syracuse, Italy

Correspondence

Alessia Coccato, Faculty of Classics, Ioannou Centre for Classical and Byzantine Studies, University of Oxford, Oxford, UK.
Email: alessia.coccato@classics.ox.ac.uk

Abstract

A collection of Hellenistic–Roman glyptics, kept at the Regional Archaeological Museum "Paolo Orsi" (Syracuse, Italy), was investigated *in situ* with portable Raman spectroscopy with the aim of assessing the viability of this approach, not only for the immediate identification of the gemstones but also for a more in-depth successive data treatment. At the same time, a corroboration of the autoptic identification of the materials, both archeological and belonging to historical collections, was looked for in order to verify and potentially correct what reported in the museum catalogue. Actually, most of the identifications could be confirmed, the glyptics being mainly made of chalcedony. Other materials found were garnet, glass, and amber. The larger group of chalcedony Raman spectra was subjected to principal components analysis treatment that, after appropriate pretreatment, resulted successful in separating spectra with higher or lower contribution of the band due to the presence of moganite and Si—OH bonds. The garnet spectra were instead subjected to quantitative study to identify the main end member. Both the quick identifications and the more detailed studies on chalcedonies and garnets were achieved thanks to the nondestructive and noninvasive investigation, directly *in situ*, with no sample preparation and minimal interference with the museum's activities.

KEYWORDS

chalcedony, garnets, PCA on Raman spectra, portable Raman spectroscopy

1 | INTRODUCTION

Portable Raman spectroscopy provides for *in situ* molecular analysis without the onerous and complicated handling of historical/archeological materials outside museums, or their disassembly.[1] As it is well known, this approach is nondestructive and can be noninvasive, not requiring sample preparation, both of which are

fundamental properties when working with museum objects.[2–4] In general, it gives excellent results on the identification of mineral species that constitute a material, and it has been largely used in the field of (applied) mineralogy/petrography,[5] including the analysis of ancient gems and precious stones in museum environments.[6–10] The advantages of using this methodology are that measurements are carried out quickly, bringing limited disruption to museum activities, offering the possibility of analyzing a large number of samples in a short time, and providing a general identification of the mineral *in situ*.[11] However, this technology has some limitations that include low spatial and spectral resolution compared with classical laboratory ones, the negative effect of environmental conditions that are not always optimal for measurements (e.g., the presence of light sources), and a greater tendency to fluorescence effects, which can cause the saturation of detector, or the impossibility of detecting Raman signals.[12]

Following a promising previous study,[13] the aim of this work is to evaluate the contribution of portable Raman spectroscopy alone to the identification of ancient gemstones in a museum context. A large number of precious materials now preserved inside the "Medagliere," a section of the Regional Archaeological Museum "Paolo Orsi" (Syracuse, Italy), were made available for this purpose. The great part of the items analyzed in this work are engraved gemstones (glyptics) of Roman–Hellenistic age, mostly loose gems, with the addition of three golden rings and a fragment of a bronze ring. Considering all the vicissitudes that these kinds of artifacts may have suffered in time, the museums require a mineralogical classification to be combined to the classical archeological and autoptic observation conducted on the materials. Therefore, the aim of answering this specific need adds to above-mentioned methodological one.

Besides the immediate mineral identification, further spectral data treatments might be required for a more thorough study of the material. For example, multivariate statistical treatment application to Raman spectra by means of principal components analysis (PCA), though quite common for the study of pigments,[14] is much less used for natural and artificial stone and gemological materials. Within the latter field, it is mainly applied to the study of amber,[13,15] obsidian[16] and synthetic glass.[17] Therefore, in this study, taking advantage from the high number of analyzed gemstones, PCA is applied to chalcedony, to assess its effectiveness and usefulness in this application of portable Raman spectroscopy.

Furthermore, many minerals, such as garnets, show solid solutions, having slightly different chemical compositions but similar structure.[18–20] The sensitivity of Raman spectroscopy to structural changes due to chemical substitutions can be exploited for determining the proportions of garnet end members, even though the different spectral resolution of portable and laboratory instrumentations must be carefully considered. Although the separation between pyrope–spessartine–almandine garnets, and grossular–andradite–uvarovite ones is straightforward and based on the appearance of the spectrum, a software has been proposed to obtain quantitative data based on the linear combination of Raman band positions of pure end members, by comparing the observed shifts to simulated ones, with a reasonable error, especially as this information is obtained in a completely noninvasive manner.[18,19,21]

Raman spectroscopy appears to be an ideal tool in corroborating the autoptic identification of archeological gemstones, providing the identification of the mineral species within minutes, directly *in situ*. The definition of the gemological materials can therefore be easily achieved without displacing the precious objects from the Museum and without sample preparation, which are both highly desirable aspects in the archeological conservation practice. Moreover, Raman spectroscopy can also easily be coupled with advanced data processing, such as PCA on the spectra of chalcedony or computational routines on the band positions of garnets.

2 | MATERIALS AND METHODS

2.1 | Samples

The materials analyzed belong to the prestigious "Medagliere" of the "Paolo Orsi" Regional Archaeological Museum (Syracuse, Italy): They are part of the museum's diverse historical collections, but the provenance of many of them remains uncertain. In the catalogue of the Museum, most of the gems subjected to analysis are registered as acquisitions, dating between the end of the 18th century and the beginning of the 19th century by several museum curators. Some of them belong to prestigious historical collections, such as the Castelluccio and the Mezio ones. On the other hand, it is worth noting that a fair number of samples are indeed archeological items found during the many excavation campaigns carried out both in Syracuse and in other areas of eastern Sicily, such as Akrai and Kamarina, until the 1970s.

A total of 73 samples was analyzed (Figure S1), 69 loose gems and 4 ring-set gems. In detail, almost all loose gems are oval in shape, except for sample 108301, which is circular; the most recurrent color is orange, present in all its shades. There are some white-colored gems (samples 22800, 24994, and 108301) and some black ones (40734, 25737, and 33484); some are polychrome, (16493,

TABLE 1 Color, optical properties, dimensions, provenance, iconographic description and notes for the 73 studied objects, as they are reported in the historical catalogue.

Catalogue number	Color	Optical properties	Dimensions	Provenance	Iconographic description	Notes
4885	Dark brown	Translucent	14 × 12 mm	Uncertain	Carnelian cabochon with smoothed bezel	Set in a gold ring with ribbon rod. Weight: 4.83 g
4900	Red-orange	Translucent, oily luster	15 mm	Megara Iblea	Carnelian scarab with warrior	
8497	Dark orange	Translucent, oily luster	10 mm	Akrai	Carnelian with bull darting to the right	
9134	Dark brown	Opaque	11 mm	Targia, SR	Carnelian with Fortune and cornucopia on the right, rudder on the left	
9481	Light orange	Translucent, oily to glassy luster	12 mm	Lentini	Carnelian with naked Hermes	
9491	Black	Translucent, oily luster	\	Syracuse, Cappuccini	Small circular garnet	Set in a gold ring with decorative plant motives engraved on the bar. Weight: 1.70 g; diam.: 18 mm.
12699	Dark orange	Translucent, oily luster	10 × 7 mm	Acquired in Akrai	Carnelian with Apollo's head	
12791	Red	Translucent, oily to glassy luster	16 × 12 mm	Syracuse	Carnelian with seated Cybele	
12806	Brown-orange	Translucent, oily luster	14 × 10 mm	Acquired in Syracuse	Carnelian with bust of Artemis (?) and quiver	
13402	Orange	Translucent, oily luster	17 mm	Acquired	Broken carnelian with philosopher's head (?)	Weight: 0.7 g
14027	Orange	Translucent, oily luster	21 × 15 mm	Camarina, Acquired in Vittoria	Carnelian scaraboid with Heracles and Athena	Thickness: 8 mm
15061	Red	Translucent, oily luster	13 mm	Acquired in Pantelleria 1895	Carnelian with figure on the right	
15216	Orange	Translucent, oily luster	12 mm	Greek Teather, Syracuse	Carnelian with eagle and lightning	
15227	Red-orange	Translucent, oily luster	17 mm	Acquired	Carnelian with winged Nike and *tainia* in hand	Weight: 1.2 g
15249	Red-orange	Translucent, oily luster	13 mm		Gem with emperor's head	
16170	Amber orange	Translucent, oily luster	12 mm	Coll. Mezio	Carnelian scarab with quadruped	Weight: 0.95 g
16493	Brown base; spotted white relief figure	Translucent base and opaque relief figure, oily to glassy luster	22 × 14 mm	Coll. Mezio	Cameo with lioness	

(Continues)

TABLE 1 (Continued)

Catalogue number	Color	Optical properties	Dimensions	Provenance	Iconographic description	Notes
16510	Scarlet red	Opaque, earthy luster	0.8 × 0.6 mm	Buscemi	Blood-red carnelian with engraved letters IIPA	
17265	Red	Translucent, oily luster	13 mm	Acquired 1897	Carnelian with seated Jupiter, a staff and Nike on the right	Weight: 0.7 g
17626	Orange	Translucent, oily luster	13 × 10 mm	Acquired 1897	Carnelian with lion	
17627	Amber orange	Translucent, oily luster	11 mm	Acquired 1897	Carnelian with nude figure on the left	
17628	Orange	Translucent, oily luster	12 mm	Acquired 1897	Elliptical carnelian with naked Mars, helmeted with shield and spear on the left and a trophy on the right	Weight: 0.55 g
17629	Straw yellow	Translucent, oily luster	12 mm	Acquired 1897	Carnelian with seated woman	
17630	Orange-red	Translucent, oily to glassy luster	13 × 10 mm	Acquired 1897	Carnelian with Athena wearing a *chiton*	
17632	Orange	Translucent, oily luster	14 mm	Guffara, Buscemi	Elliptical carnelian with trophy	
17633	Light orange; white area	Translucent, oily luster	11 mm	Guffara, Buscemi	Carnelian with female figure	
17634	Canary yellow; light orange in edges	Translucent, oily luster	10 mm	Guffara, Buscemi	Carnelian with bird	
17635	Ivory, orange edge	Translucent, resinous to glassy luster	11 mm	Uncertain	Carnelian with bearded head and *petasos*	Weight: 0.45 g
19023	Dark Orange	Translucent, oily luster	12 × 6 mm	Syracuse, acquired	Carnelian with old man (Filottete?)	
20145	Orange	Translucent, oily luster	12 × 8 mm	Agrigento	Carnelian with barbarian head	
20509	Red	Translucent, oily luster	14 × 11 mm	Syracuse	Carnelian with Athena Promachos	Chipped
21119	Dark brown	Translucent, oily luster	12 mm	Acquired in Taranto	Yellow carnelian with hand holding spikes	Weight: 0.6 g
21120	Brown	Opaque, oily luster	12 mm	Acquired in Taranto 1901	Carnelian with bird	
21690	Brown	Opaque, oily luster	12 mm		Agate scarab	
22501	Orange	Translucent, oily luster	18 mm	Acquired	Carnelian with engraved woman's head (Modern?)	

TABLE 1 (Continued)

Catalogue number	Color	Optical properties	Dimensions	Provenance	Iconographic description	Notes
22502	Orange	Translucent, oily luster	20 mm	Acquired	Carnelian with engraved woman's head. Modern	
22503	Orange-straw yellow	Translucent, oily luster	17 mm	Acquired	Carnelian with Heracles' head (?) covered with eagle's *spolia*	
22504	Ivory-orange	Translucent, oily luster	17 mm	Acquired	Oblong carnelian with engraved woman's head. Modern	
22731	Coral red	Translucent, oily to resinous luster	8 × 7 mm	Acquired in Palazzolo 1903	Elliptical carnelian with naked Hermes	
22732	Dark brown	Opaque, oily sheen	11 mm	Akrai	Orange elliptic carnelian with a woman crouching and two spikes	
22800	White	Translucent, oily luster	18 mm	Camarina	Onyx (?) chalcedony (?) with Jupiter seated on the right	
22801	Orange	Translucent, oily luster	8 mm	Acquired	Carnelian bezel with female head	Bronze ring fragment. Size 16 mm
23572	Dark orange	Opaque	16 × 12 mm	Palazzolo	Carnelian with Cybele sitting on lion	
23585	Amber orange	Translucent, oily luster	13 × 9 mm	Acquired in Taormina?	Scarab (?)	
24468	Orange	Translucent, oily luster	\	Acquired from a family in Noto	Carnelian with naked young man	
24536	Dark brown	Opaque, oily sheen	10.5 mm	Acquired in Catania 1905	Carnelian gemstone with Eros holding a syringe in outstretched hands and behind a column	
24994	White	Translucent, glassy luster	9 mm	Acquired in Palazzolo	Light glass with dog figure	
25241	Scarlet red	Translucent, oily luster	12 × 9 mm	Acquired in Paternò 1906	Oval carnelian engraved with Iside holding a situla in her lowered right hand and a sistrum in her upper left hand	Set in gold ring with enlarged ribbon rod. Weight: 13.6 g
25332	Orange-brown	Translucent, oily luster	14 mm	Acquired in 1906	Carnelian with Eros holding the bow	Consumed

(Continues)

TABLE 1 (Continued)

Catalogue number	Color	Optical properties	Dimensions	Provenance	Iconographic description	Notes
25737	Black, central white band	Opaque	18 mm	Coll. Castelluccio ancient	Black stone (glass paste?) with central vein engraving of naked Aphrodite with cherub	
25784	Light orange	Translucent, oily luster	22 × 11 mm	Coll. Castelluccio (modern?)	Elliptical carnelian with Eros and Psyche hugging	
25791	Light orange	Translucent, oily luster	20 mm	Coll. Castelluccio (modern?)	Elliptical carnelian with Eros walking towards cornucopia	
25849	Black brown	Translucent, oily luster	16 × 10 mm	Coll. Castelluccio	Carnelian with naked Poseidon and trident	Height: 3 mm
25968	Light orange, yellow edge	Translucent, oily luster	14 mm	Coll. Castelluccio (modern?)	Elliptical carnelian with Eros shooting his bow towards a heart on a column	Inscription: AV PLVS ADROIT
26386	Red	Translucent, oily luster	13 × 10 mm	Found in "Piazza d'armi" (Syracuse)	Carnelian with mendicant	
29137	Red-orange	Translucent, oily luster	10 mm	Akrai	Globular type beetle with Pegasus	
33484	Light gray with central white band	Translucent, glassy to oily luster	16 mm	Lentini	Scaraboid with female head	
34042	Amber orange	Translucent, oily luster	12 mm	Centuripe	Carnelian scarab with backward facing dog	
34638	Ivory-orange	Translucent, oily luster	16 × 11 mm	Acquired in Calabria	Elliptical carnelian with Victory seated on rock playing double flute	
34651	Red-carmine	Translucent, oily luster	12 mm	Acquired	Carnelian with two draped figures and a spike	
36140	Dark brown	Opaque, oily luster	14 mm	Acquired	Carnelian with naked Nike (profile) with a crowned head to the right	
36264	Orange, white	Translucent, oily luster	11 × 7 mm	Acquired	Cameo with bust of Eros	
36268	Amber orange	Translucent, resinous luster	13.5 mm	Acquired	Carnelian with Nike crowning figure with cornucopia	Splintered in the center
37184	Dark orange	Translucent, oily luster	17 mm	Syracuse	Scarab with naked Heracles and bow	Splintered

TABLE 1 (Continued)

Catalogue number	Color	Optical properties	Dimensions	Provenance	Iconographic description	Notes
37375	Red	Translucent, oily luster	18 mm	Camarina	Scarab with centaur	
39221	Amber orange	Translucent, oily luster	15 mm	Acquired in Catania 1918	Scarab with centaur arms raised	
39743	Red	Translucent, oily luster	16 mm	Acquired	Carnelian with Artemis huntress and inscription	
40732	Orange, straw yellow areas	Translucent, oily luster	16 × 14 mm	Acquired	Carnelian with two naked warriors	Inscription: L. PVBLICIVS
40733	ivory with two white bands	Translucent, oily luster and glassy outside	16 mm	Acquired	Onyx with seated woman and cornucopia, a figure in the left, Kalathos at her feet	
40734	Black	Opaque	15 mm	Acquired	Onyx with Ceres-Abudantia (?) with cornucopia, spikes and rampant piglet (?)	
48231	Dark orange	Translucent, oily luster	25 × 15 mm	Acquired	Engraved amber with complex scene (Hermes and Aphrodite?)	
108300	Light orange	Translucent, oily luster	9 × 6 mm	Camarina 1966	Small carnelian scarab with stylised Pegasus	Weight: 0.55 g
108301	White	Translucent, oily luster	16 mm	Camarina 1971, from "Casa dell'Iscrizione"	Glass gem	Weight: 2.56 g

36264, and 40733). Almost all of them have very fine engravings of mythological figures, animals or busts of important people of the time (mainly Roman), and scenes of everyday life, while few have inscriptions (16510 and 25968). Lastly, eight samples are scarabs with engravings on the flat side.

As for the set gems, three of them are individually mounted on gold rings, and one on a fragment of a bronze ring (sample 22801). Also in this case, there is a strong variation in the colors of the gems, ranging from brown to deep red. In particular, samples 4885, 9491, and 22801 are circular, the first two have no engravings, and sample 25241 is oval and shows an engraved figure. For further details about the gems, such as color, optical properties, size, place of purchase or finding, and iconographic description, please refer to Table 1. Pictures of all the samples are reported in Figure S1. A few examples are shown in Figure 1, while Figures 2–6 show the gems as well as their Raman spectra.

2.2 | Techniques

The analyses were performed with a portable i-Raman® Plus Raman spectrometer by B&W Tek (Newark, DE, USA). This device includes a 785-nm diode laser with adjustable output power (maximum nominal power: 455 mW, settable from a minimum of 3 mW through variations of 1%), to avoid thermal effects. It is provided with a thermoelectrically cooled quantum charge-coupled device detector and covers the spectral range between 65 and 3400 cm^{-1}, with a maximum nominal spectral resolution of 3.5 cm^{-1}.

The spectrometer is coupled, via optic fiber cables, to a probe (BAC102-785E B&W Tek) that allows the positioning of the laser beam on the desired portion of the sample. This has a distance regulator to guarantee a sufficient focus on the sample, which is provided by a flat quartz lens, and it has a focal point diameter in the plane (spot) of 90 μm. The instrumentation is controlled by the dedicated software BWSpec®. The analyses, carried out with the room lights switched off and after a preliminary dark spectrum acquisition, were generally set at three accumulations of 30 s with 10% laser power; when necessary, these parameters were adjusted according to the requirements of the specific sample.

A preliminary identification of the mineral species allowed to separate chalcedony and garnet spectra. Chalcedony spectra were cut in the 435–525 cm^{-1} region, smoothed (Savitsky–Golay function), baseline-subtracted (multipoint baseline) and decomposed using LabSpec® 5. The same software was also used to obtain first and second derivative of the spectra. The spectra and their derivative curves were subjected to PCA using Orange 3.29 software,[22] where they were normalized to the maximum.

In order to increase the knowledge of the analyzed garnets and, more specifically to obtain a molar composition without the use of additional analytical techniques, the spectra were extracted between 100 and 1000 cm^{-1}, a line-segment baseline correction and a decomposition of the bands was performed using the GaussLauren function, by using LabSpec®. The obtained peak positions

FIGURE 1 Photographs of some of the 73 analyzed glyptics, 11 loose engraved gemstones, and 1 set in a bronze ring (fragment, 22801). *Source*: Photographs are shown by concession of "Assessorato dei Beni Culturali e dell'Identità Siciliana" and should not be further duplicated, not even in part.

were then given as input to the latest available version of Miragem, the MatLab routine created by Bersani et al. for the quantitative assessment of garnets.[19,23] The routine is designed to work with 3 to 6 band positions, which allowed to process even spectra of lower quality acquired with the portable spectrometer.

3 | RESULTS

In the following sections, the results obtained will be grouped according to the type of attribution, presenting new identifications of previously unassigned materials first, then the changed attributions which confuted the description reported in the catalogue, and finally the results that confirmed the historical information. In general, most of the spectra showed a wavy noise and artifacts that might be confused with Raman signals, due to both the multilayered filter and problems with the dark subtraction that can be encountered with this kind of instrumentation. A reference spectrum acquired without any sample was used in order to avoid this confusion and consider true Raman signals only.
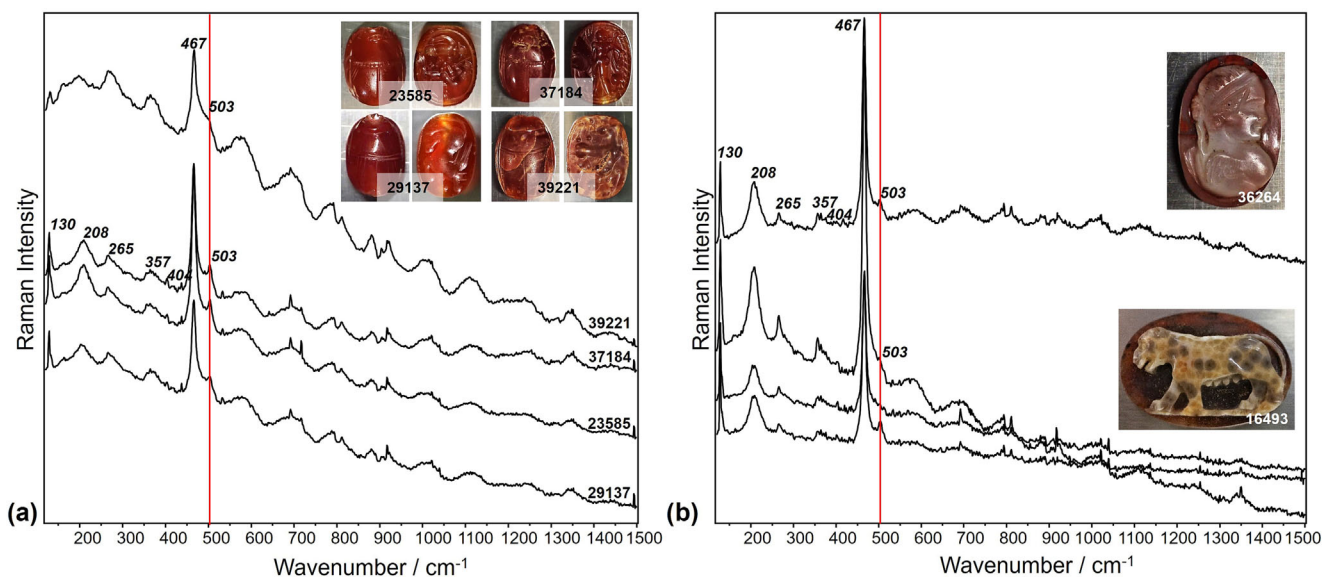

FIGURE 2 Representative Raman spectra (as acquired) of four scarab gemstones (a) and two cameos (b). Spectra are stacked for clarity.
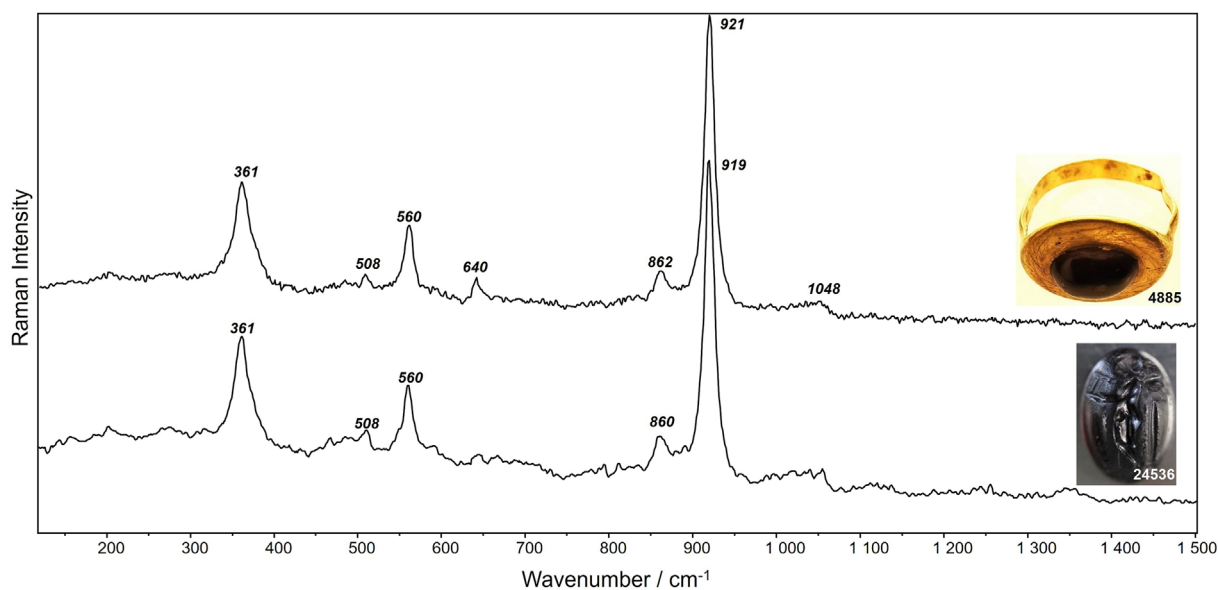

FIGURE 3 Representative Raman spectra (as acquired) of a ring-set and a loose gemstone. Spectra are stacked for clarity.
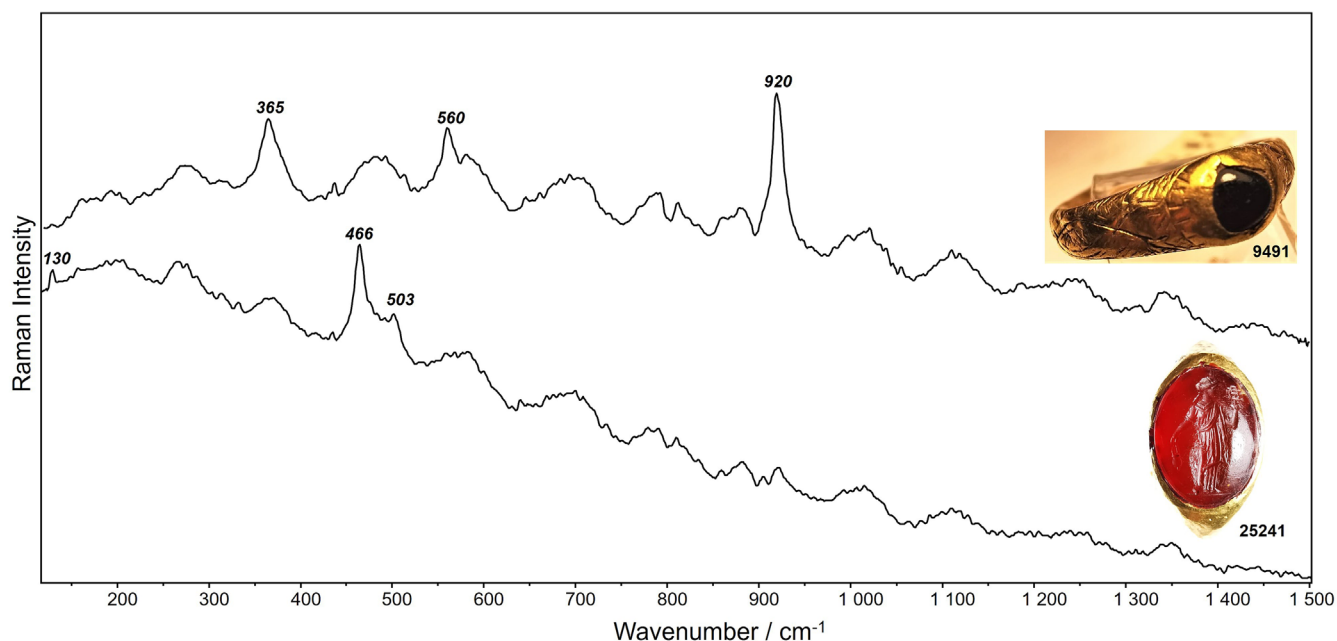
FIGURE 4 Representative Raman spectra (as acquired) of 2 ring-set gemstones. Spectra are stacked for clarity.
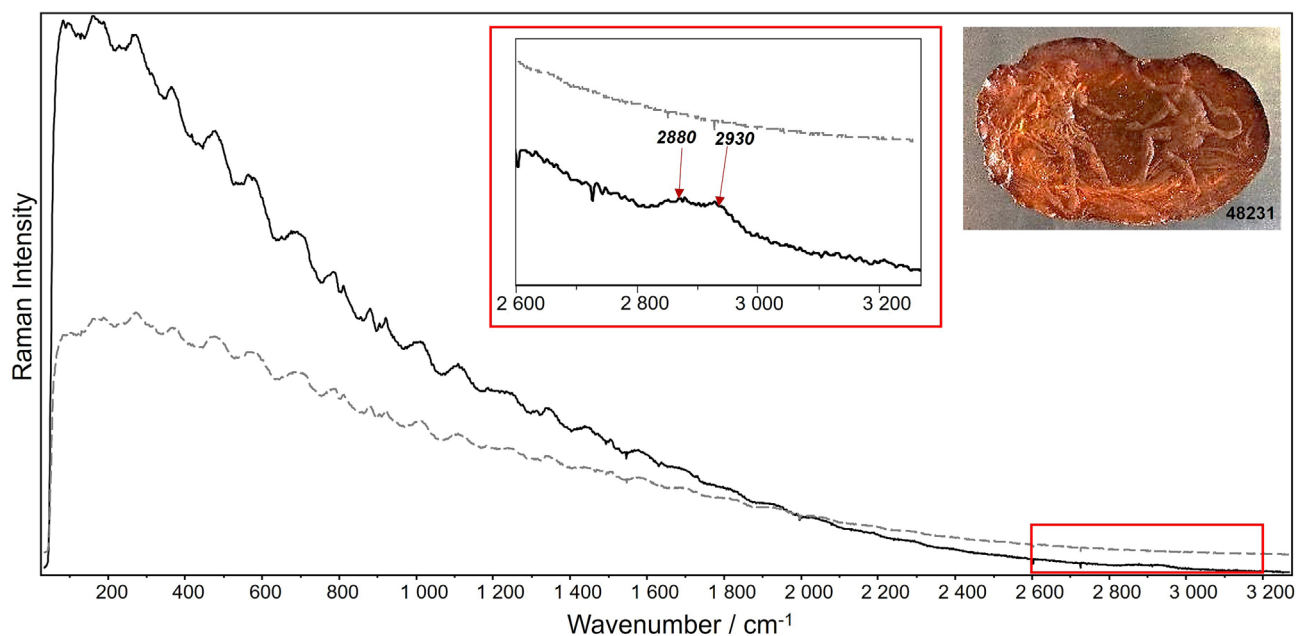

FIGURE 5 Representative Raman spectrum (as acquired) of 48231 gemstone (black solid line) and reference spectrum acquired without any sample (dashed gray line); in the inset: close-up on the 2600–3300 cm^{-1} region. Spectra are stacked for clarity.

3.1 | New attributions

Nine loose gemstones were catalogued as "cameo," "scarab," or "gem" without any attempt of autoptic identification of the constituting material. All the materials gave a Raman spectrum with peaks at about 130, 208, 357, 404, 467, and 503 cm^{-1}, where the latter signal leads to the identification of the material as a microcrystalline

form of silica, that we can generally define as chalcedony[24] (Figure 2). This latter band has been for a long time uniquely attributed to the presence of the silica polymorph moganite in chalcedony,[24,25] but nowadays, the prevailing hypothesis assigns it to the combination of the moganite peak at 500–501 cm^{-1} and nonbridging Si—O vibration of silanole at 503 cm^{-1}.[26,27] In this study, a distinction could not be performed, due to the spectral

resolution of the portable instrumentation. The Raman spectra acquired on different areas of the precious cameo with lioness belonging to the Mezio collection, showed variable intensities of the approximately 503 cm^{-1} band (Figure 2b). This could be due to the different composition of the variously colored spots of the lioness mantle, even though the precise position of the analyzed spot cannot be stated.

3.2 | Changed attributions

Two wrong attributions reported in the catalogue regarded the ring 4885 and the loose gemstone 24536, both believed to be made of carnelian. Actually, the Raman spectra exhibited for both samples signals around 361, 508, 560, 640, 862, 920, and 1048 cm^{-1}, attributable to garnets of the pyralspite series.[19] Furthermore, a gemstone catalogued as carnelian (20145) did not give any Raman spectrum of chalcedony. On the other hand, it showed the presence of a strong and broad photoluminescence band between 1100 and 2100 cm^{-1}, with a maximum at about 1360 cm^{-1}, corresponding to approximately 879 nm considering the excitation wavelength at 785 nm, and probably due to the presence of Nd^{3+}.[28] The same has been found for other materials classified as "glass"; therefore, this latter attribution cannot be excluded in this case.[8]

3.3 | Confirmed attributions

The given attribution could be confirmed for the other two rings of the selection: For the 9491, garnet signals were found while for 25241, the principal signals of chalcedony at 130, 466, and 503 cm^{-1} were revealed (Figure 4).

Except for the materials that could not be identified due to fluorescence, all the other gemstones catalogued as carnelian/agate/onyx gave spectra analogous to those shown in Figure 2; therefore, the general definition of chalcedony can be given and the autoptic identification confirmed. Other confirmations concern a black and white glass paste gem (25737), where again no signals of crystalline phases were found but a broad photoluminescence band, and an amber gemstone (48231). The spectrum of the latter at first view did not seem to show any Raman signals (see Figure 5); at a closer inspection, by comparing it with the reference spectrum acquired without any sample, bands at 2880 and 2930 cm^{-1} can be noticed and cannot be confused with the wavy instrumental noise (Figure 5): These are typical of CH$_2$ and CH$_3$ stretching vibrations in amber.[29,30]

4 | DISCUSSIONS

The following sections aim at evaluating the possibility of performing data treatment even if the spectral quality is affected by fluorescence, filter noise, environmental noise and low spectral resolution, and at summarizing the performance of the used portable Raman instrument in the *in situ* analysis of ancient gemstones.

4.1 | Chalcedony spectral processing: decomposition and PCA

The Raman spectra of chalcedony were here considered with the aim of studying the contribution of the band typical of microcrystalline silica. Götze et al.[31] suggested a method to quantify moganite percentage. This is obtained by building a calibration curve with the ratio of the intensities of the principal Raman peaks of moganite and α-quartz versus the moganite content measured with X-ray diffraction (XRD). It has already been reported that the 503 cm^{-1} Raman band is probably not due to the moganite contribution only.[26,27] Moreover, the limits of the use of a portable instrumentation instead of a micro-Raman had to be carefully considered in this case. On the one hand, using a measuring head without a magnifying objective allowed to obtain a relatively large angle of irradiation, simultaneously analyzing many different scattering geometries and avoiding crystallographic orientation effects.[31] On the other hand, the instrumental noise could affect the intensity of the bands (see for example Figures 2 and 4). First of all, of the 53 spectra of chalcedony, the best 35 were chosen avoiding those in which the wavy noise was prevailing on the Raman signals. Second, after baseline subtraction and extraction of the region 435–525 cm^{-1}, the spectra were decomposed to isolate the main bands at about 465 and 503 cm^{-1}. As observed in Figure 6, where two extreme examples are reported, a further component at about 470 cm^{-1} had to be added in order to achieve a good fitting and exclude the contribution of the wavy noise of the multilayer filter. According to Götze et al.,[31] the background increases with the increase of moganite content. In our study, no relation was found between the approximately 470 and 503 cm^{-1} bands intensities, thus ascribing the former band to filter noise rather than background. After decomposition, the ratio of the main bands areas was calculated as percentage: A$_{503}$/A$_{465}$ (%). The values ranged from a minimum of 5.9% to a maximum of 55.6%, which, according to the above-mentioned calibration curve,[31] would correspond to a wide range of approximately 25%–75% of moganite in a system constituted of moganite and α-quartz only.
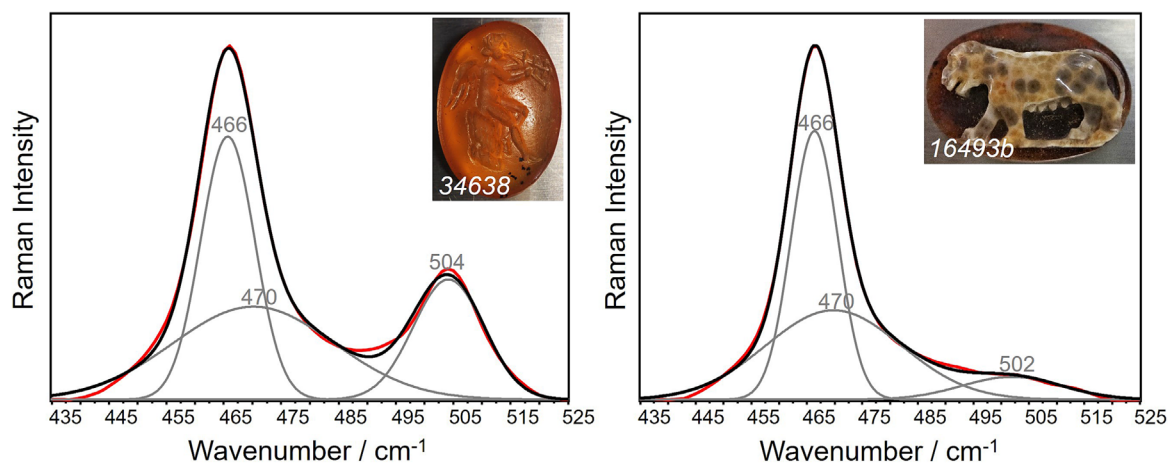
FIGURE 6 Representative baseline-subtracted Raman spectra of chalcedony samples cut in the region 435–525 cm^{-1} and subsequently decomposed.

Another kind of approach was attempted for discriminating spectra with different intensities of the 503 cm^{-1} band avoiding spectral decomposition. Spectra were appropriately de-spiked, smoothed, cut, baseline-subtracted and normalized (Figure 7a), as required by multivariate statistical analysis preprocessing.[32] Subsequently, PCA was performed. Values of the first principal component (PC1; explained variance = 85%) were plotted against the area ratio calculated as described above. The obtained graph (Figure 7d) shows a positive trend, with an ill-defined correlation. Deviations from the norm could be due to the spectral region between 475 and 490 cm^{-1}, which accounts for the noise presence. According to literature, PCA performed on first[33] or second derivative[34,35] Raman spectra of different kinds of materials gives better results than when performed on the original data, as derivation reduces the contribution of broad features. Actually, it can be observed that in the first (Figure 7b) and second (Figure 7c) derivative, the differences among the samples in the above-mentioned spectral region are almost eliminated (compare the region within markers in Figure 7a–c). Consequently, correlations of PC1 values (explained variance for first derivative = 78%; for second derivative = 80%) with decomposed peaks areas ratios appear much clearer (Figure 7e,f). In both graphs, few samples show a higher contribution of the 503 cm^{-1} band, while the larger, main group of samples exhibits values included between 6% and 30% (see Figure 7f), that is, 25%–60% of moganite content.[31] These values are higher than those measured with synchrotron radiation XRD on analogous glyptics from Vigna Barberini (Palatine Hill, Rome, Italy).[36] On the other hand, moganite-rich chalcedony (content up to 70 ± 10%) has been found in Indian basalts,[37] and it must be reminded that Pliny mentioned India among the

carnelian suppliers.[36] However, due to (1) the mentioned issues about the attribution of the 503 cm^{-1} Raman band, with a probable overestimation of moganite, (2) the wide concentration range obtained, and (3) the many other possible sources cited by Pliny, no sharp conclusions can be drawn on this respect, but probably XRD and/or elemental analysis would be requested.[38]

If PC2 and PC3 are added to the PCA treatment on the second derivative Raman spectra, the explained variance reaches 93% of the total variance (PC2 = 9%, PC3 = 4%). As observed in the loadings diagram (Figure 8), PC3 mainly accounts for the artifact signal at 470 cm^{-1} while PC2 considerably varies also for the other two main bands. Therefore, PC2 was plotted against PC1 (Figure 8). Though no clusters are visible, observations can be made looking at the PC values. Samples of the series "17," among which those coming from Guffara and Buscemi are all characterized by a positive PC1, as well as most of the other samples of certain archeological origin, but unknown provenance. Samples 22502, 22503, and 22504 all have negative PC1 values while sample 22501 has positive ones. Samples 22502 and 22504 are most probably modern, as well as 25784 and 25791 falling close to them. PC1 values are linked to different A_{503}/A_{465} ratios, which might potentially suggest a different source of chalcedony for modern samples.

4.2 │ Garnet spectral decomposition for quantitative study

Even though the spectra collected *in situ* with a portable Raman are affected by interferences of various nature, as already mentioned, and by the intrinsic limitations of
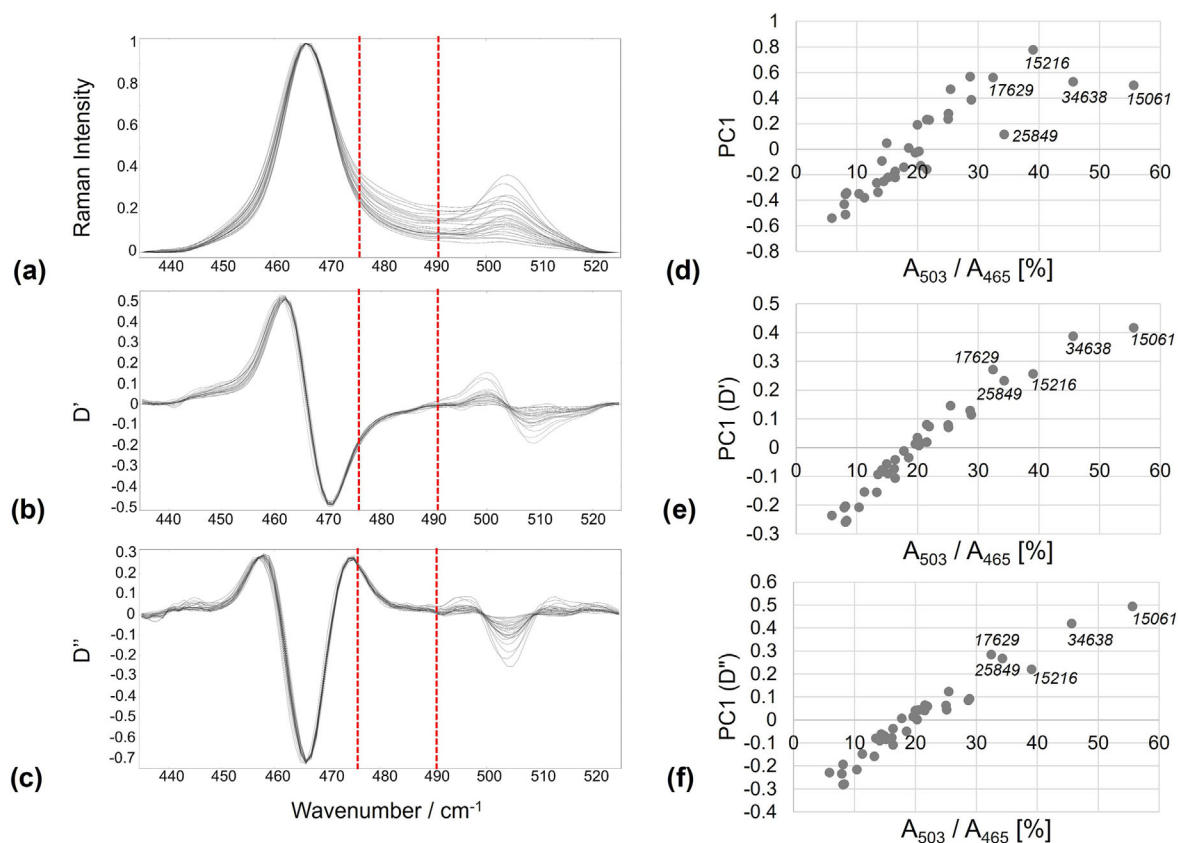
FIGURE 7 Smoothed, cut, baseline-subtracted and normalized Raman spectra of 35 chalcedony samples in the 435–525 cm^{-1} region (a) with their first (b) and second (c) derivatives; plots of the first principal component (PC1) against the A_{503}/A_{465} (%) for the treated Raman spectra (d) and for their respective first (e) and second (f) derivative.
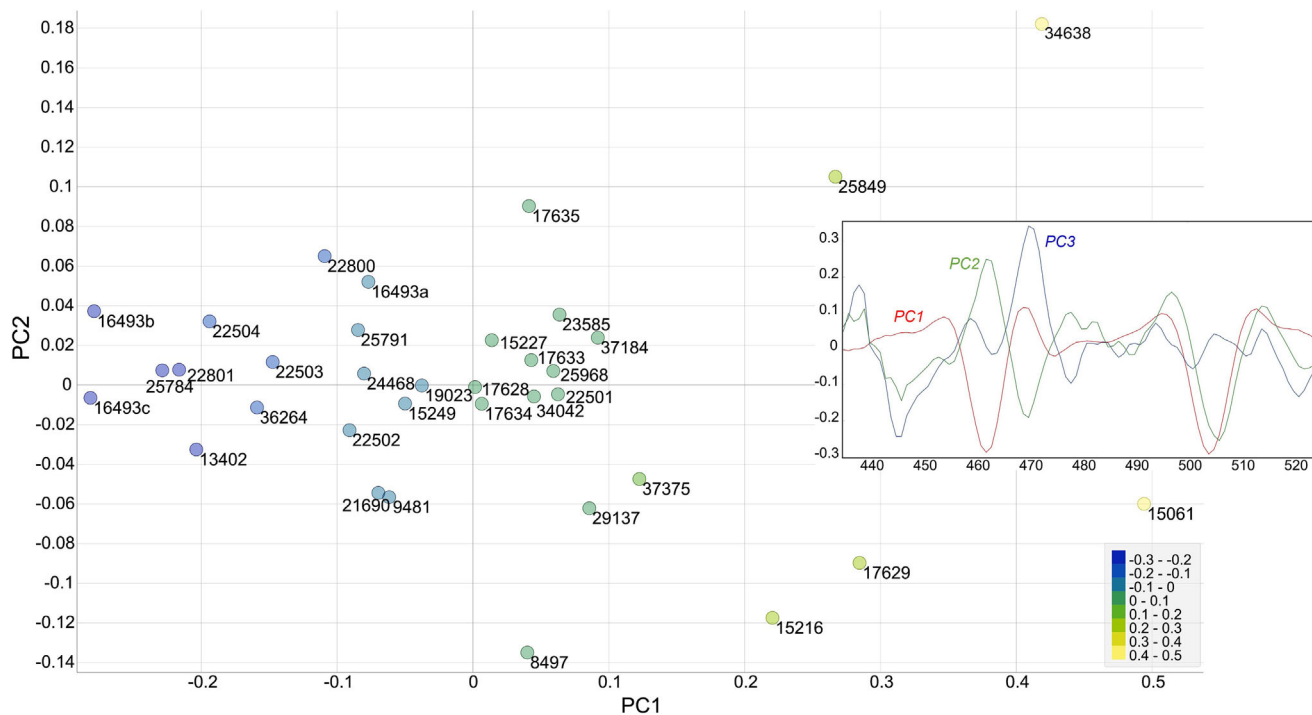

FIGURE 8 PC1 versus PC2 scores plot (PC1 is also indicated by the color scale) of the second derivative of 35 chalcedony Raman spectra in the 435–525 cm^{-1} region and loadings diagram of the first three principal components.

instrumental spectral resolution, it is possible to apply a simple computational routine to the spectra of garnets, to obtain their composition in terms of end members.[18] Miragem[19] has demonstrated its effectiveness in the completely nondestructive chemical analysis of garnets of geological[39] and gemological interest.[13] The basic principle is that garnets' Raman bands can be considered as a linear combination of weighted band positions, the weight being the proportion of a specific end member, and the band position being that of the pure end member.[18] The observed band positions are used as input. Here the routine is used with only 3 to 4 peak positions, instead of the optimal 5 to 6 required. Pyralspite garnets do have weak bands, such as the 220 and the 860 cm^{-1} ones, which are sometimes not appearing in the spectrum, and also show a doublet at approximately 360–370 cm^{-1}, whose separation is strongly affected by the instrumental spectral resolution.

Nevertheless, the simulated Raman band positions match well with the measured ones, used as input (Table 2), and allow to assess the main component of the mixture (Table 3), with an error as low as 10%.[19]

From such computational approach, it looks like besides pyrope, which is the recurring main component, the second component in this set is grossular. Nevertheless, all three garnets display a deep red color, almost black in the case of 24536. The apparent dissimilarity of sample 9491 from the other two is probably because its composition was estimated based on three Raman bands only. Such spectra (and compositional ranges) are in good agreement with literature on the pyrope–grossular series,[40] which were also tested with Miragem, providing very good results in the range 100% to 60% pyrope. Such a composition points to ultrabasic parent rocks, such as peridotites, eclogites, or kimberlites.[41] Results obtained with Miragem on garnets studied in a previous *in situ* campaign[13] show, again, pyrope as the main component (between 70% and 80%), but with spessartine as the second one. From visual inspection, the color of such gemstones is much lighter, supporting a different composition.

Gem quality pyropes in Europe occur in Scotland and Portugal (Cr poor), and in Bohemia and Norway (Cr rich).[42] For the Greco–Roman period, however, there is limited compositional data available compared with later periods,[43] which invariably points out, for pyropes, to the Portuguese mines of Monte Suímo, which were exploited in Roman times, as mentioned by Pliny the Elder.[42] Garnets of comparable composition (∼55%–80% pyrope, 5%–15% grossular + spessartine, and 10%–30% almandine) have been recognized in Etruscan, Hellenistic, and Roman (mid-1st BC to late 1st century AD) contexts.[43] Even though there is no information on chromium content, the historical context indicates this as the most likely source for the gemstones.

4.3 | General remarks

If we consider the Raman results as a whole (Figure 9), more than 68% of the total analyses gave a confirmation of the autoptic identification, corroborating the archeological interpretation, with the confirmed vast majority of chalcedony. There were 12 samples (15%) not identified due to the prevailing fluorescence effect that could not be abated notwithstanding the changing of the operational parameters. On the other hand, the total of successful new attributions and the corrected ones exceeds 16%. Within the new identification, a clear predominance of chalcedony is once more registered. In the changed identifications, instead, garnet prevailed, originally misidentified as carnelian.

TABLE 2 Raman band positions obtained after spectral processing, Raman bands simulated by Miragem and difference.

Sample ID	Used bands			
4885	362.7	561.3	862.7	920.1
Simulated	362.6	560.8	862.6	920.1
Difference	0.1	0.4	0.1	0.0
9491	366.0	559.9	—	920.3
Simulated	363.6	560.8	—	919.6
Difference	2.4	−0.9	—	0.7
24536	362.3	560.8	862.8	919.2
Simulated	362.2	560.7	862.5	919.9
Difference	0.1	0.1	0.2	−0.7

Note: All values in cm^{-1}.

TABLE 3 Molar composition of the analyzed garnets obtained from the processing of Raman spectral data.

| Sample ID | Approximate composition as contributions of end members | | | | |
	Almandine	Pyrope	Spessartine	Andradite	Grossular
4885	4%	84%	<1%	<1%	12%
9491	<1%	86%	<1%	<1%	14%
24536	6%	82%	<1%	<1%	12%
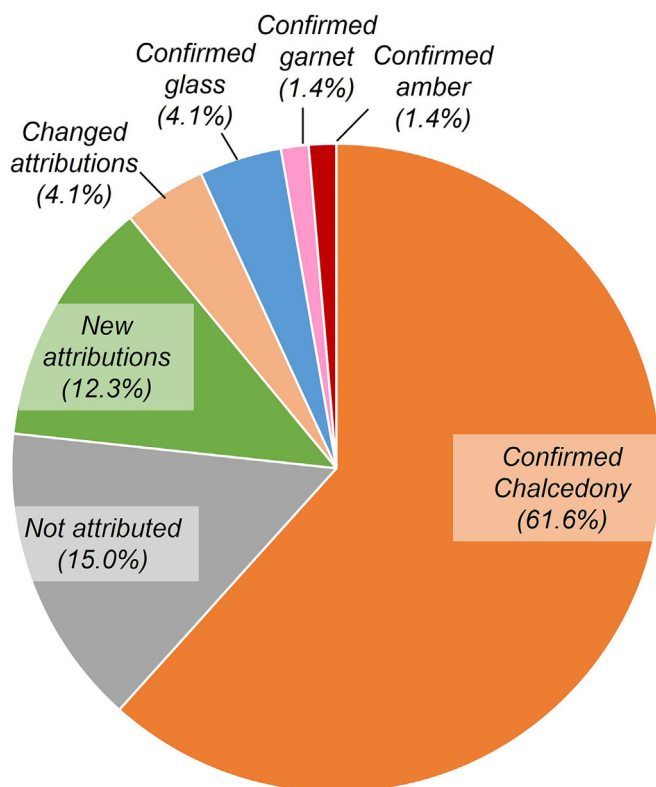
FIGURE 9 Aerogram of the Raman results on the 73 analyzed gemstones.

the application of PCA to spectra from portable Raman instrumentation, which is most rarely found in literature, especially for this kind of materials. PCA data were then successfully cross-checked with those resulting from bands decomposition: PC1 variation in accordance with 503 cm^{-1} band intensity in the chalcedony spectra demonstrated that this approach could replace the longer and more complex band decomposition. Besides, PCA distinguished most of the archeological samples from most of the probably modern ones based on the A_{503}/A_{465} ratio. Furthermore, the reasonable estimates of the main end member (relative error lower than 10%) of garnets are a promising opportunity for a fast but systematic approach to label checking in different kinds of museums. On the other hand, it appears clear that the archeometric results should be intersected with the archeological information, without which, as it happens in this case for many historic private collections and acquisitions, discussions about the choice of materials in the past and the understanding of their commercial routes are difficult.

5 | CONCLUSIONS

The *in situ* campaign conducted by means of portable Raman spectroscopy alone at the Regional Archaeological Museum "Paolo Orsi" (Syracuse, Italy) underlined the ability of this technique of obtaining meaningful results from totally nondestructive and noninvasive investigations on historical samples as such, without displacing them from the Museum. In fact, the study was successful for the identification of 85% of the analyzed Hellenistic–Roman glyptics. The identification was corrected for about 4% of the gemstones, among which a precious gold ring with garnet was previously mistaken for carnelian. The speediness of the analysis allowed limiting in time the interference with the Museum's activities. The use of a 785-nm laser surely reduced the possible fluorescence with respect to higher-energy excitation sources. The possible problems caused by filter noise were limited comparing the samples' spectra with a reference one and performing spectral treatment. This was possible even if spectra appeared affected by instrumental weaknesses thanks to an appropriate pretreatment. In detail, band decomposition or, in alternative, first/second derivative of chalcedony spectra allowed to abate the noise contribution. The high number of chalcedony spectra was exploited to test

CONFLICT OF INTEREST STATEMENT
The authors declare no known conflicts of interest.

DATA AVAILABILITY STATEMENT
The data are available from the corresponding author upon reasonable request.

ORCID
Maria Cristina Caggiani https://orcid.org/0000-0001-8475-1175
Marco Cavarra https://orcid.org/0009-0008-4210-4517
Germana Barone https://orcid.org/0000-0003-0822-2436
Alessia Coccato https://orcid.org/0000-0002-6641-2820
Paolo Mazzoleni https://orcid.org/0000-0002-7281-923X

REFERENCES

[1] D. Bersani, P. P. Lottici, *Anal. Bioanal. Chem.* **2010**, *397*, 2631.

[2] P. Vandenabeele, J. Tate, L. Moens, *Anal. Bioanal. Chem.* **2007**, *387*, 813.

[3] P. Vandenabeele, H. G. M. Edwards, J. Jehlička, *Chem. Soc. Rev.* **2014**, *43*, 2628.

[4] J. Jehlička, A. Culka, *Anal. Theor. Chim. Acta* **2022**, *1209*, 339027. https://doi.org/10.1016/j.aca.2021.339027

[5] J. Jehlička, A. Culka, D. Bersani, P. Vandenabeele, *J. Raman Spectrosc.* **2017**, *48*, 1289.

[6] G. Barone, D. Bersani, J. Jehlička, P. P. Lottici, P. Mazzoleni, S. Raneri, P. Vandenabeele, C. Di Giacomo, G. Larinà, *J. Raman Spectrosc.* **2015**, *46*, 989.

[7] K. Osterrothová, L. Minaříková, A. Culka, J. Kuntoš, J. Jehlička, *J. Raman Spectrosc.* **2014**, *45*, 830.

[8] D. Lauwers, A. Candeias, A. Coccato, J. Mirao, L. Moens, P. Vandenabeele, *Spectrochim. Acta - Part a Mol. Biomol. Spectrosc.* **2016**, *157*, 146.

[9] G. Economou, E. Konstantinidi-Syvridi, I. Kougemitrou, M. Perraki, D. C. Smith, *Bull. Geol. Soc. Greece* **2010**, *43*, 804.

[10] P. Colomban, G. S. Franci, F. Koleini, *Heritage* **2021**, *4*, 524.

[11] G. Barone, D. Bersani, J. Jehlicka, P. Mazzoleni, S. Raneri, *Period. di Mineral.* **2015**, *208*, 27.

[12] J. Jehlička, A. Culka, P. Vandenabeele, H. G. M. Edwards, *Spectrochim. Acta - Part a Mol. Biomol. Spectrosc.* **2011**, *80*, 36.

[13] G. Barone, P. Mazzoleni, S. Raneri, J. Jehlička, P. Vandenabeele, P. P. Lottici, G. Lamagna, A. M. Manenti, D. Bersani, *Appl. Spectrosc.* **2016**, *70*, 1420.

[14] F. Casadio, C. Daher, L. Bellot-Gurlet, *Top. Curr. Chem.* **2016**, *374*, 374.

[15] G. I. Badea, M. C. Caggiani, P. Colomban, A. Mangone, E. D. Teodor, E. S. Teodor, G. L. Radu, *Appl. Spectrosc.* **2015**, *69*, 1457.

[16] R. McMillan, M. Amini, D. Weis, *J. Archaeol. Sci. Rep.* **2019**, *28*, 102040.

[17] P. Colomban, A. Tournie, L. Bellot-Gurlet, *J. Raman Spectrosc.* **2006**, *37*, 841.

[18] D. C. Smith, *Spectrochim. Acta - Part a Mol. Biomol. Spectrosc.* **2005**, *61*, 2299.

[19] D. Bersani, S. Andò, P. Vignola, G. Moltifiori, I. G. Marino, P. P. Lottici, V. Diella, *Spectrochim. Acta - Part a Mol. Biomol. Spectrosc.* **2009**, *73*, 484.

[20] E. H. Nickel, *Mineral. Petrol.* **1992**, *46*, 49.

[21] A. Culka, J. Jehlička, *J. Raman Spectrosc.* **2019**, *50*, 262.

[22] J. Demsar, T. Curk, A. Erjavec, C. Gorup, T. Hocevar, M. Milutinovic, M. Mozina, M. Polajnar, M. Toplak, A. Staric, M. Stajdohar, L. Umek, L. Zagar, J. Zbontar, M. Zitnik, B. Zupan, *J. Mach. Learn. Res.* **2013**, *14*, 2349.

[23] D. Bersani, S. Andò, P. Vignola, I. G. Marino, P. P. Lottici, in AIP Conference Proceedings, **2009**, pp. 35–43.

[24] K. J. Kingma, R. J. Hemley, *Am. Mineral.* **1994**, *79*, 269.

[25] K. A. Rodgers, W. A. Hampton, *Mineral. Mag.* **2003**, *67*, 1.

[26] P. Schmidt, L. Bellot-Gurlet, V. Leá, P. Sciau, *Eur. J. Mineral.* **2014**, *25*, 797.

[27] P. Schmidt, L. Bellot-Gurlet, A. Slodczyk, F. Fröhlich, *Phys. Chem. Miner.* **2012**, *39*, 455.

[28] C. M. MacRae, N. C. Wilson, *Microsc. Microanal.* **2008**, *14*, 184.

[29] G. I. Truică, N. Ditaranto, M. C. Caggiani, A. Mangone, S. C. Liţescu, E. D. Teodor, L. Sabbatini, G. L. Radu, *Chem. Pap.* **2014**, *68*, 15.

[30] G. Barone, D. Capitani, P. Mazzoleni, N. Proietti, S. Raneri, U. Longobardo, V. Di Tullio, *Appl. Spectrosc.* **2016**, *70*, 1346.

[31] J. Götze, L. Nasdala, R. Kleeberg, M. Wenzel, *Mineral. Petrol.* **1998**, *133*, 96.

[32] R. Gautam, S. Vanga, F. Ariese, S. Umapathy, *EPJ Tech. Instrum.* **2015**, *2*, 8. https://doi.org/10.1140/epjti/s40485-015-0018-6

[33] N. Navas, J. Romero-Pastor, E. Manzano, C. Cardell, *J. Raman Spectrosc.* **2010**, *41*, 1196.

[34] F. Pozzi, S. Porcinai, J. R. Lombardi, M. Leona, *Anal. Methods* **2013**, *5*, 4205.

[35] P. Vandenabeele, L. Moens, *Analyst* **2003**, *128*, 187.

[36] E. Gliozzo, N. Grassi, P. Bonanni, C. Meneghini, M. A. Tomei, *Archaeometry* **2011**, *53*, 469.

[37] G. Parthasarathy, A. C. Kunwar, R. Srinivasan, *Eur. J. Mineral.* **2001**, *13*, 127.

[38] E. Gliozzo, D. J. Mattingly, F. Cole, G. Artioli, *J. Archaeol. Sci.* **2014**, *52*, 218.

[39] S. Andò, D. Bersani, P. Vignola, E. Garzanti, *Spectrochim. Acta - Part a Mol. Biomol. Spectrosc.* **2009**, *73*, 450.

[40] W. Du, B. Han, S. M. Clark, Y. Wang, X. Liu, *Phys. Chem. Miner.* **2018**, *45*, 197.

[41] S. M. Suggate, R. Hall, *Geol. Soc. Spec. Pub.* **2014**, *386*, 373.

[42] H. A. Gilg, J. Hyrsl, in *Rouges Noirs. Rubis, Grenat, Onyx, Obsidienne et autres minéraux rouges, noirs dans l art et l archéologie*, (Ed: J. Toussaint), Société archéologique de Namur, Brussels **2014** 144.

[43] L. Thoresen, K. Schmetzer, *J. Gemmol.* **2013**, *33*, 201.

SUPPORTING INFORMATION

Additional supporting information can be found online in the Supporting Information section at the end of this article.